Chemistry Europe

AWARD

Nominate a Worthy Chemist Chemistry Europe Award

Subject:
chemistry for sustainability, energy, materials, environment

Consists of:
prize money amounting to EUR 10,000, certificate

Deadline:
November 1, 2022

Click here for more info & nomination

Materials Science inc. Nanomaterials & Polymers

Effective Heterogeneous Fenton-Like degradation of Malachite Green Dye Using the Core-Shell Fe_3O_4@SiO_2 Nano-Catalyst

Nafis Mahmud,[a] Abdelbaki Benamor,*[a] Mustafa S. Nasser,[a] Muneer M. Ba-Abbad,[a] Muftah H. El-Naas,[a] and Abdul Wahab Mohammad[b, c]

In this study, the application of the core-shell Fe_3O_4@SiO_2 nano-catalysts for fenton-like degradation of malachite green dye has been presented. The nano-catalysts were prepared using a combination of solvothermal and sol-gel techniques and characterized using XRD, FTIR, SEM/EDX, TEM and VSM techniques. The effects of various reaction parameters on the degradation of malachite green dye using the prepared nano-catalysts were investigated. The optimal condition for pH, catalyst dosage and H_2O_2 amount were found to be at 6.7, 15 mg and 50 μL, respectively. Under the optimized conditions, a degradation efficiency of 96.18% for malachite green dye was achieved using the catalyst within 30 minutes at 303 K with a pseudo first order rate constant of 0.1102 min^{-1}. The plausible mechanism for MG degradation was determined to be the combination of adsorption and simultaneous decomposition via formation of hydroxyl radicals. The performance of the nano-catalyst was compared with other fenton-like catalysts reported in the literature. Finally, the magnetic properties of the Fe_3O_4@SiO_2 catalysts was utilized for its successful recovery and application in multiple degradation cycles.

1. Introduction

Water pollution from industrial wastewater effluents has become a growing environmental concern of the world. Of the various compounds being discharged, organic dyes are an important class of pollutant that can contaminate both the surface and ground water.[1] Organic dyes are readily used in textile, leather, paper production and food technology industries to color their respective products. Consequently, a huge portion of the effluents originating from these industries contains organic dyes. Fazal et al.[2] reported that an estimate of 2.8 million tons of dyes is being discharged around world per annum. Malachite green (MG) is one such dye that is being readily discharged from the industries. It is commonly used for dying cotton, silk, paper, leather and for producing paint and ink for printing purposes.[3] It is further used as a coloring agent for various food products.[4] However, studies have shown that MG dyes are highly carcinogenic and harmful for aquatic environment.[5] They are easily miscible in water and alcohol and once consumed they can disrupt the reproductive and immune systems.[6,7] Moreover, studies have shown that MG dyes are environmentally persistent and cannot be easily removed.[8] Therefore, the removal malachite green dye from the industrial wastewaters is of paramount importance for the safety and well-being of both the aquatic and human environment.

In the past few years, the use of advanced oxidation processes (AOPs) have emerged as attractive option for remediation of organic pollutants from wastewater.[9,10] In this AOPs, highly reactive radicals are produced which then helps in oxidizing the organic pollutants.[11] Unlike the traditional activated sludge process, AOP's can handle a wide variety of pollutants and are now readily being employed in both laboratory and industrial scale.[12] Of the several possible routes for AOP, fenton reaction is the mostly widely deployed method which involves the decomposition of H_2O_2 to hydroxyl and hydroperoxyl radicals in presence of Fe^{2+} ions.[13] However, their successful implementation depends several factors like maintaining an acidic pH of 3 and requiring stochiometric amount of the Fe^{2+} ions. Moreover, it can generate large amounts of iron sludge.[14,15] Therefore, the application of heterogenous fenton catalysts instead of the traditional fenton catalyst is becoming increasing popular as they can easily overcome these drawbacks.[16,17]

Among the several heterogenous fenton-like catalysts studied in the literature, Fe_3O_4 could spontaneously catalyze the hydrogen peroxide under various experimental conditions.[18,19] However, successful fenton-like oxidation re-

[a] N. Mahmud, Dr. A. Benamor, Dr. M. S. Nasser, Dr. M. M. Ba-Abbad, Prof. M. H. El-Naas
Gas Processing Centre, College of Engineering, Qatar University, 2713, Doha, Qatar
E-mail: benamor.abdelbaki@qu.edu.qa
[b] Prof. A. W. Mohammad
Chemical Engineering Programme, Faculty of Engineering and Built Environment, Universiti Kebangsaan Malaysia, 43600 Bangi, Selangor Darul Ehsan, Malaysia
[c] Prof. A. W. Mohammad
Centre for Sustainable Process Technology (CESPRO), Faculty of Engineering and Built Environment, Universiti Kebangsaan Malaysia, 43600 Bangi, Selangor Darul Ehsan, Malaysia

Supporting information for this article is available on the WWW under https://doi.org/10.1002/slct.202003937

quires introduction of external energy. For instance, Liu et al.[20] reported that the catalytic activity of the Fe_3O_4 NP's for activating peroxymonosulfates to degrade acid orange 7 was significantly enhanced through ultrasound irritation. Carvallho et el.[21] applied the Fe_3O_4 NP's of different grain size in photodegradation of rhodamine B. They concluded that the degradation significantly increased with the decrease in the grain size of the nanoparticles. However, other findings indicated that the surface modification of the Fe_3O_4 NP's can facilitate the fenton-like degradation phenomena without the requirement of any external source of energy. Zhang et al.[22] reported that the carbon encapsulated Fe_3O_4 NP's could successfully degrade methyl blue dyes under acidic pH without requiring any external energy supply. Studies have shown that Incorporation of SiO_2 or TiO_2 coating to Fe_3O_4 NP's can even shift the optimal pH for degradation to near neutral conditions. For example, Wang et al.[23] applied Fe_3O_4@SiO_2@C for the degradation of the methyl blue and achieved decent degradation over a pH rage to 3 to 9. Also, Liu et al.[24] applied Fe_3O_4@TiO_2@C nanocomposites for degradation of MB dye at neutral pH. However, it is to be noted the aforementioned composites were mostly prepared using Fe_3O_4 NP's that were synthesized via co-precipitation. Nanoparticles prepared via this method tends to be of non-uniform morphology and form aggregates. This results in loss of active sites and the diffusion of peroxide to the catalyst surface requires significantly longer time. Thus, effecting the overall catalytic activity of the nanocomposites.

Despite, the promising characteristics of the surface modified Fe_3O_4 NP's in degradation of methyl blue and rhodamine B dyes, not many studies have focused on its application in degradation of malachite green dye. Therefore, the main objective of this study is to investigate the application of core-shell Fe_3O_4@SiO_2 nano-catalysts in fenton-like degradation of malachite green dyes. The Fe_3O_4@SiO_2 nano-catalysts were synthesized via a combination of solvothermal and sol-gel process. Use of hydrothermal method allowed in synthesizing Fe_3O_4 NP's of distinct morphology, while, sol-gel technique ensured the application of clear SiO_2 coatings on each Fe_3O_4 grains which may ensure in low loss of catalytic active sites. The as-prepared Fe_3O_4@SiO_2 nano-catalysts were characterized using X-ray Diffraction (XRD), Fourier transform infrared spectroscopy (FTIR), Scanning Electron Microscopy with energy dispersive x-ray spectroscopy (SEM/EDX), Transmission Electron Microscopy (TEM) and vibrating sample magnetometer (VSM) techniques. Batch experiments were conducted to determine the optimum conditions for various operating parameters like pH, catalyst dosage and H_2O_2 amount for degradation of MG dye using the as prepared Fe_3O_4@SiO_2 nano-catalysts. The possible mechanisms involved in the degradation process are briefly discussed. Moreover, kinetics study was also conducted under the optimum condition to determine rate constant for MG degradation. Finally, the performance of the nano-catalysts was compared to other recently reported fenton catalysts. Overall, the findings of this study are expected to provide significant insights for application Fe_3O_4@SiO_2 nano-catalysts for degradation of MG dyes and its potentials to be used in the field of industrial wastewater treatment.

2. Results and discussion

2.1. Catalyst Characterization

The crystalline structure and phase composition of the Fe_3O_4 and Fe_3O_4@SiO_2 particles was analyzed using XRD apparatus. As shown in Figure 1, the XRD patterns of the both samples mainly composed of the characteristic peaks of Iron Oxide [JCPDS No.19-0629] as indicated the sharper peaks noticed at 2θ values of 30°, 35.3°, 43°, 53.3°, 56.8°, and 62.5° corresponding to the (220), (311), (400), (422), (511), and (440) planes, respectively.[25] However, in case of Fe_3O_4@SiO_2 particles, a broad peak was observed between the 2θ values of 22–28

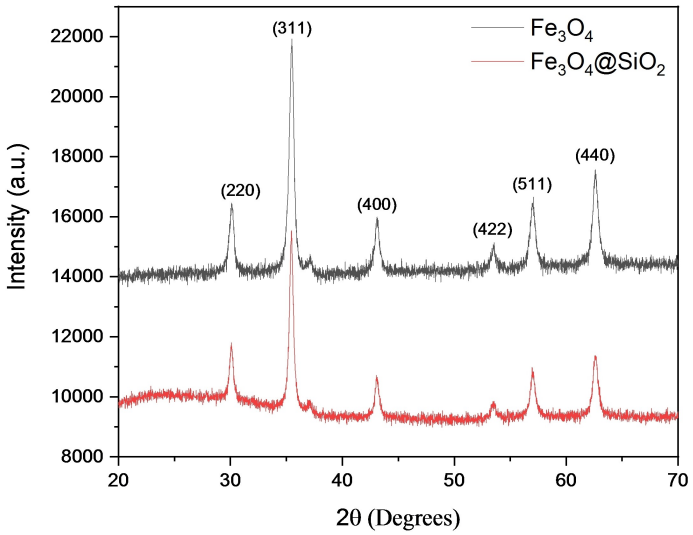

Figure 1. XRD patterns of Fe_3O_4 and Fe_3O_4@SiO_2.

which corresponds to the peak of amorphous SiO_2. Furthermore, an overall reduction of the baseline in terms of intensity was also observed, which indicated the formation of SiO_2 shell around the Fe_3O_4 particles reducing its peak intensities. The XRD patterns were used to estimate the average particle size of the nanoparticles using Scherrer's equation given by the equation 3.

$$d = \frac{k\lambda}{\beta cos\theta} \quad (1)$$

Here, the terms k, λ, β and θ represents the Scherrer constant, the wavelength of Cu Ka X-ray (1.5406 Å); full width at half-maximum (FWHM) of the XRD peaks, and the Bragg diffraction angle, respectively. Using this equation the average particle size of the Fe_3O_4 and $Fe_3O_4@SiO_2$ particles was estimated to be around 184 and 189 nm, respectively.[27]

The FTIR spectrums of the Fe_3O_4 and $Fe_3O_4@SiO_2$ particles are given in the Figure 2. The peak around 540 cm^{-1} observed in the FTIR spectrum of the Fe_3O_4 and at 560 cm^{-1} observed in the FTIR spectrum of the $Fe_3O_4@SiO_2$ particles corresponded to the Fe–O bond of thebulk Fe_3O_4 nanoparticles.[28,29] Additionally, the spectrum of the $Fe_3O_4@SiO_2$ nano-catalysts, contained a sharp peak at 1080 cm^{-1} which represents the formation of Si–O–Si bond along with a shoulder at around 950 cm^{-1} representing the formation of Si–OH.[30–32] These peaks further affirm the formation silica shell around the magnetic core.

The SEM images for $Fe_3O_4@SiO_2$ nano-catalysts is presented in Figure 3(a) and Figure 3(b). It was observed that the nano-catalysts were spherical in structure. Each sphere appeared to form out of agglomerations of smaller crystals. Depending on the number of smaller crystals agglomerated, a wide variation in the size of the spheres was observed. With the exception of few smaller sphere whose diameters was less than 50 nm, most of the nano-catalyst had a diameter range of 100–250 nm. The image could not provide any insight on the presence of SiO_2, however, EDX analysis of the confirmed the presence Si element. Based on EDX data Figure 3 (c), the as prepared $Fe_3O_4@SiO_2$ nano-catalyst primarily contained three major elements namely; Iron (Fe), Silicon (Si) and Oxygen (O). Of the three elements present within the nano-crystal, the Iron (60.79%) and Oxygen (34.15%) were found to be dominant compared to the Silicon (4.09%). The high content of Fe and O indicates that the observed spheres primarily contained Iron oxide.

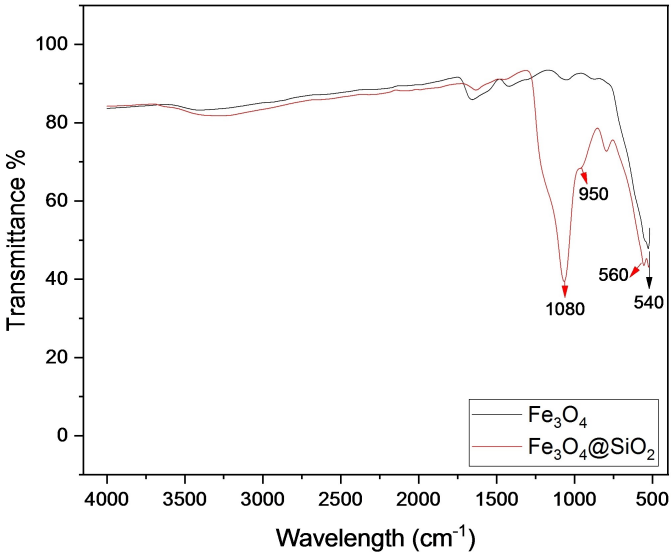

Figure 2. FTIR spectrum of Fe_3O_4 and $Fe_3O_4@SiO_2$.

The core-shell structure of the $Fe_3O_4@SiO_2$ nano-catalysts was confirmed through the elemental distribution observed using HRTEM-STEM analysis coupled with EDS elemental mapping as shown in Figure 4. The elemental mapping Figure 4b–e correspond to the area in Figure 4a. The core of the nano-catalyst was expected to be composed of iron oxide only which was affirmed from the identical elemental mappings obtained for Fe and O (Figure 4b and 4d). On the contrary, the elemental mapping of Si (Figure 4c) showed their presence as hollow shells. Upon overlapping the three elements Fe, O and Si (Figure 4e), Fe and O together appeared to form the core of the nano-catalysts while the outer layer composed of the blue silicon layer. Hence, confirming the core-shell structure of the catalysts.

The magnetic hysteresis loops of the Fe_3O_4 and $Fe_3O_4@SiO_2$ particles are given in the Figure 5 a) at room temperature. Both of the nanoparticles, showed superparamagnetic behavior with very narrow hysteresis, which could be largely attributed to the presence of ultrafine Fe_3O_4 nanocrystals within their structure. The saturation magnetism of the of the Fe_3O_4 nanoparticles was 57.95 $emu.g^{-1}$. But the saturation magnetism of the $Fe_3O_4@SiO_2$ particles was evidently lower compared to the former at 22.20 $emu.g^{-1}$. The lower magnetizing values stems from the immobilization of amorphous silica, thus, reducing the overall magnetic strength of the $Fe_3O_4@SiO_2$ particles. However, it is to be noted that the nano-catalysts still exhibited great magnetic properties suggesting their suitability for magnetic recovery as shown in Figure 5 b) and subsequent reuse.

2.2. Effect of pH

The pH of the solution is a crucial factor in fenton-like catalytic degradation reactions. The degradation efficiency of the malachite green dye was investigated between the range of 3–7 while maintaining the experimental factors such H_2O_2 amount, Catalyst dosage and temperature at 50 μL, 15 mg and 303 K, respectively. Commonly, the most efficient pH for fenton like degradation of malachite green dye is reported to be at an acidic pH of 3.[3,9,33–35] However, in case of the as prepared $Fe_3O_4@SiO_2$ nano-catalysts, the degradation efficiency of the malachite green was low at pH of 3 (efficiency 10.99%). The degradation efficiency progressively increased the with the increase in pH and reached its maximum at near neutral condition (pH 6.7, efficiency 96.18%). The phenomena is primarily caused by the presence of SiO_2 shells of the nano-catalyst as they are known to push fenton-like reactions

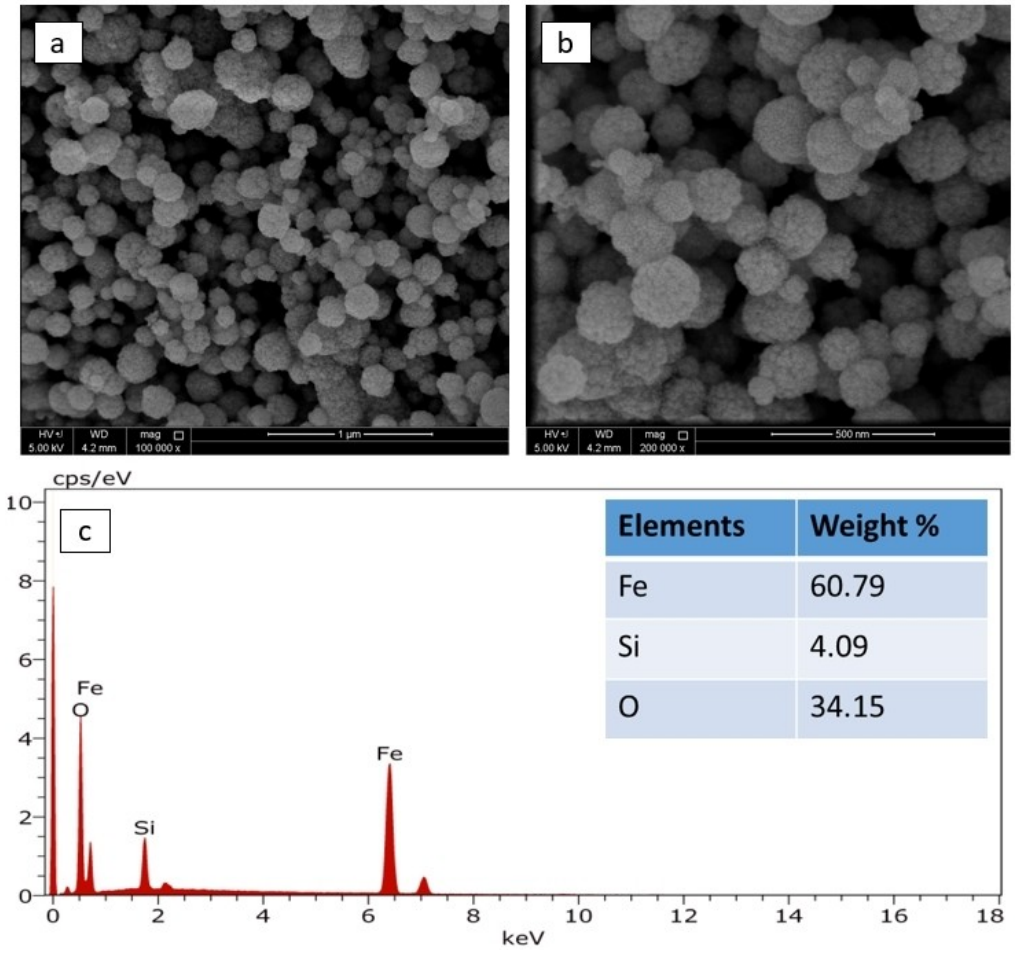

Figure 3. The SEM image at a) 1 μm and b) 500 nm and c) EDX analysis of the as prepared Fe_3O_4@SiO_2.

towards neutral pH.[12,19,36] SiO_2 contains multiple hydroxyl groups which can chelate with Fe^{2+} and Fe^{3+} ions of the Fe_30_4 core forming a rather weak chelation. This chelation formed promotes the Fenton reactions to occur under neutral conditions.[37] Furthermore, it confirms the influence of the core-shell Fe_3O_4@SiO_2 nano-catalysts and displays its merit to be used under near neutral pH. Therefore, based on the investigations, a pH of 6.7 was chosen as optimum pH for the fenton-like degradation of MG experiments.

2.3. Effect of Catalyst Dosage

A series of experiments were performed to investigate the role of the amount of core-shell Fe_3O_4@SiO_2 nano-catalysts on the fenton like degradation of the MG dye. The dose of the nano-catalysts was varied between 5 to 25 mg for 30 minutes while maintaining the experimental factors such H_2O_2 amount, pH and temperature at 50 μL, 6.7 and 303 K, respectively. As depicted in Figure 6b, the degradation efficiency progressively increased with the increasing amount of nano-catalysts. This is because higher dose of Fe_3O_4@SiO_2 nano-catalysts resulted in an increase of adsorption sites, subsequently providing more active sides to activate H_2O_2 to generate more hydroxyl radicals.[38,39] Around 78.31% of the malachite green dye degraded at 5 mg dosage. The degradation efficiency improved with addition of 5 more grams to 90.80%. At 15 mg dose of Fe_3O_4@SiO_2 nano-catalysts, the degradation efficiency further improved to 96.77%. No significant improvement was observed upon further addition of the nano-catalyst due to self-scavenging of the hydroxyl radicals by the nano-catalyst.[40] Hence, 15 mg was set as the optimum dose of the Fe_3O_4@SiO_2 nano-catalyst.

2.4. Effect of H_2O_2

Since the amount of H_2O_2 plays a key role in the generation of hydroxyl radicals,[41] it directly effects the degradation efficiency of fenton-like reactions.[42,43] A number of experiments were performed to investigate the impact of H_2O_2 dose on the degradation of MG dye. The experiments were performed by varying the peroxide dose between 25 to 100 μL for 30 minutes; while, maintaining the experimental factors such Catalyst dosage, pH and temperature at 15 mg, 6.7 and 303 K, respectively. Similar to the catalyst dose, the degradation of

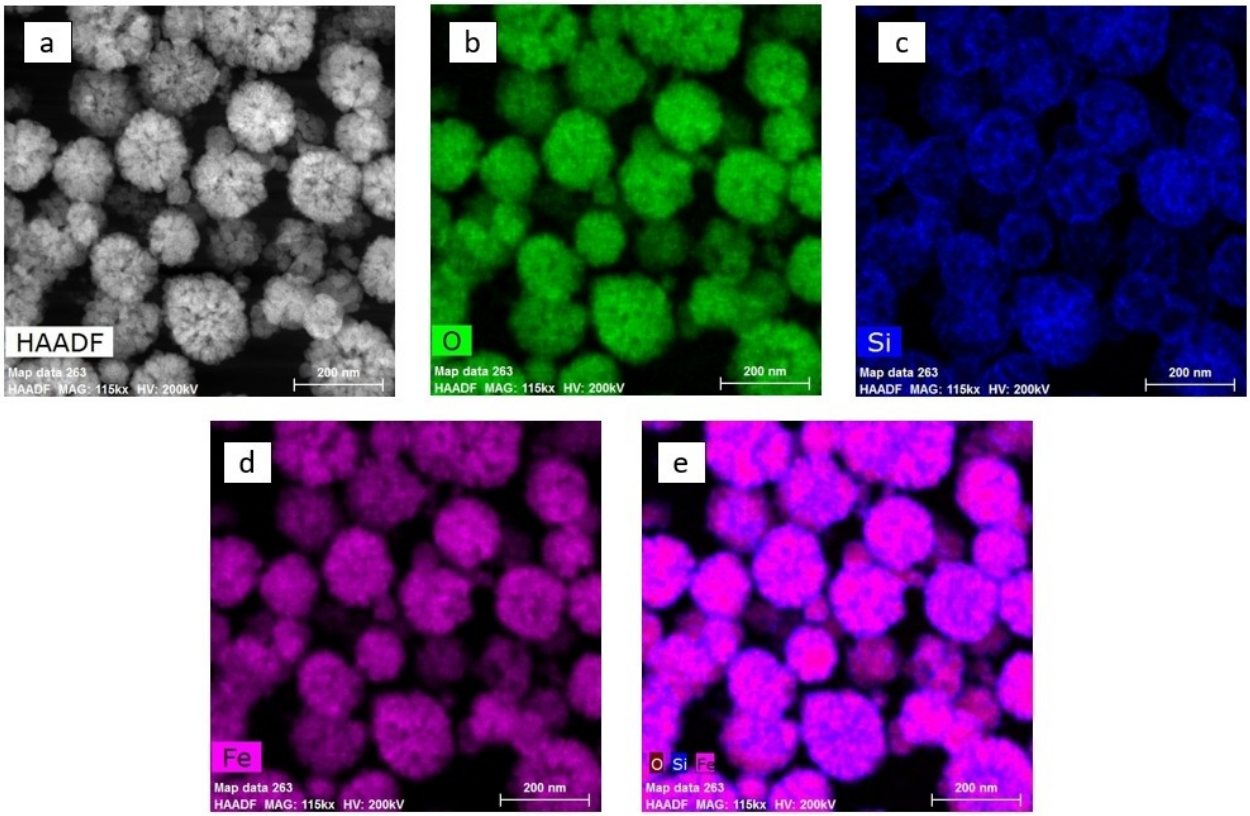

Figure 4. a) HAADF- STEM phase mapping of Fe_3O_4@SiO_2. EDS elemental mapping of b) O c) Si d) Fe and e) Fe–O–Si performed on the area of the selected region of STEM image.

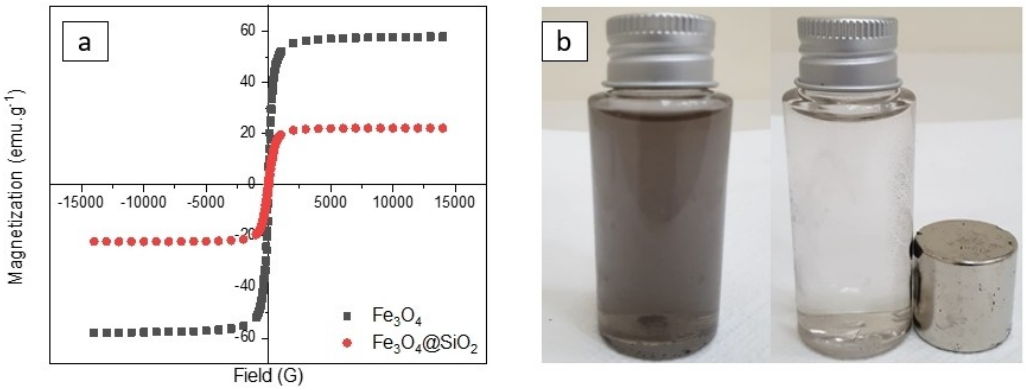

Figure 5. a) The vibrating sample magnetometer curves of the Fe_3O_4 and Fe_3O_4@SiO_2 nanoparticles and a) photograph of the magnetic separation of Fe_3O_4@SiO_2 nanoparticles.

MG dye increased with the increasing amount of H_2O_2 as shown in figure 6c. Control experiments performed without H_2O_2 showed a degradation of 33.60% at the end of the experimental time, due to adsorption on the surface of the nano-catalyst.[44] However, around 89.03% of the MG dye were removed with the addition of only 25 µL of the H_2O_2. Peroxide dose of 50 µL improved degradation efficiency to 96.18%. No further significant improvement in the degradation of MG dye was observed upon addition of more H_2O_2. Therefore, 50 µL was set as the optimum amount of peroxide for the degradation experiments.

2.5. Fenton-like Degradation of Malachite Green and Plausible Degradation Pathway

Using the optimum conditions for pH, Catalyst dosage and H_2O_2 amount, experiments were performed to investigate the fenton-like degradation of malachite green using the

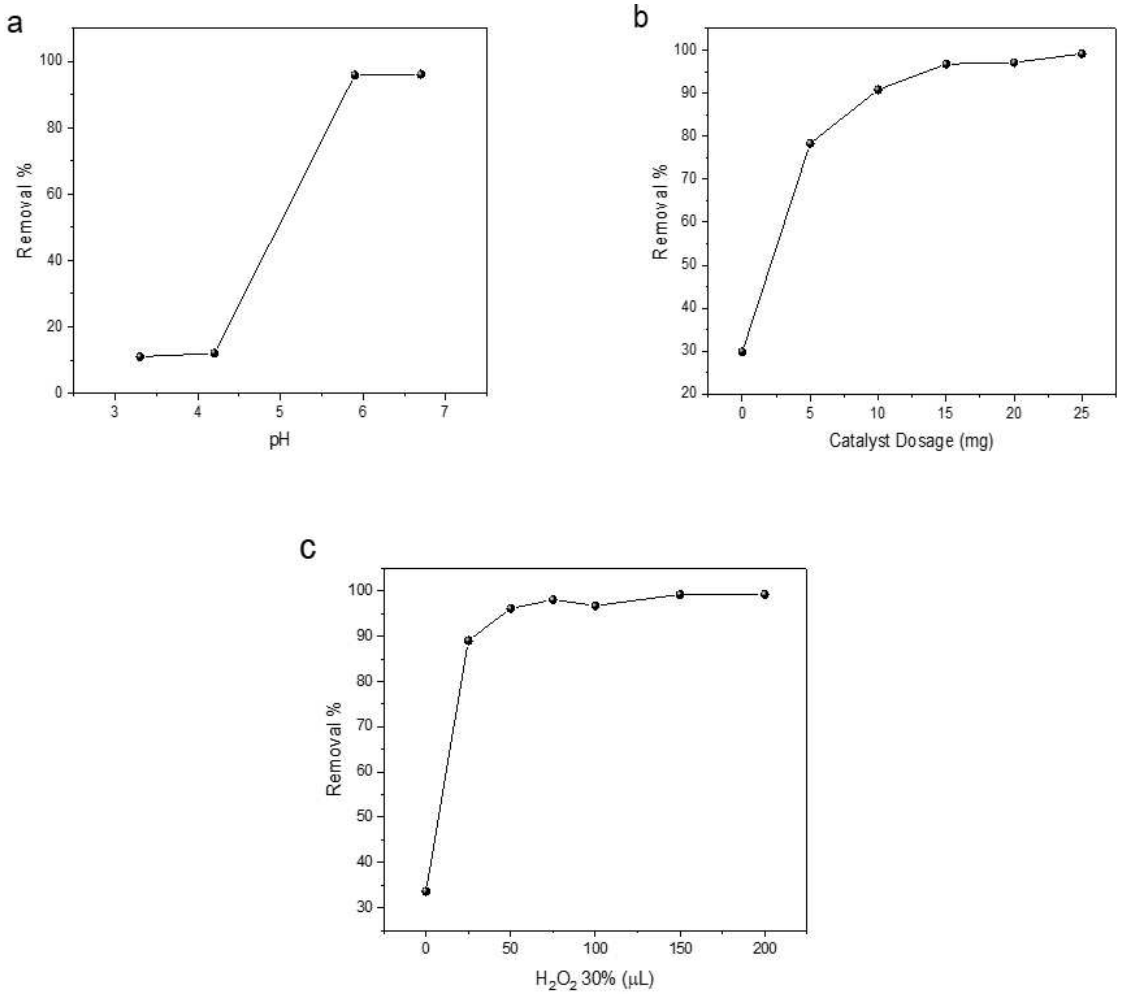

Figure 6. Effect of various influencing factors: a) Ph, b) Catalyst Dosage and c) H_2O_2 amount on the fenton-like Degradation of MG dye at 303 K.

Fe_3O_4@SiO_2 nano-catalysts at 303 K. As depicted in the Figure 7, four different systems were compared under the similar conditions, namely; H_2O_2 system, Fe_3O_4@SiO_2 system, Fe_3O_4-H_2O_2 system and Fe_3O_4@SiO_2-H_2O_2 system. Evidently, the Fe_3O_4@SiO_2 nano-catalysts was the most effective in catalyzing the fenton-like degradation of MG dye. The H_2O_2 decomposed to form the radicals in presence of the Fe_3O_4@SiO_2 nano-catalysts which in turn oxidized the MG dye. Almost a complete degradation of the MG dye was achieved within 30 minutes with a degradation efficiency of 96.18%. While the other three systems exhibited lower degradation efficiencies within the same time frame at 13.88%, 32.38% and 20.24% for H_2O_2, Fe_3O_4@SiO_2 and Fe_3O_4-H_2O_2 systems, respectively. The low degradation efficiencies observed in these systems is mainly caused by the near neutral pH and lack of external energy.[12,36] The effectiveness of the Fe_3O_4@SiO_2 nano-catalysts in degradation of the malachite green dye was further confirmed by the evaluation of the degradation kinetics using the equation (2). The obtained k_1 value of 0.1102 min^{-1} was much higher than k_1 values of 0.0052, 0.0502 and 0.0143 min^{-1} obtained for the H_2O_2, Fe_3O_4-H_2O_2 and Fe_3O_4@SiO_2 systems, respectively. Among the three systems with low degradation kinetics, it was noticed that the k_1 values of the Fe_3O_4@SiO_2 system without the H_2O_2 was almost three times higher than the other two systems, indicating that the MG dye could be absorbed by the Fe_3O_4@SiO_2 catalyst. Therefore, based on these observations, the high kinetics observed for the Fe_3O_4@SiO_2-H_2O_2 systems, can be attributed for the following reasons. As the SiO_2 shell of Fe_3O_4@SiO_2 nano-catalyst adsorbed the MG dye, it resulted in pre-concentration of the MG dye around the iron oxide cores.[45,46] As a result, more hydroxyl radicals could reach the MG dye before its self-destruction. Moreover, studies have shown that the electron transfer between iron to the MG readily occurs in presence of SiO_2.[47,48] Therefore, these two factors combined with the formation of weak chelation (section 3.2) has resulted in high degradation efficiency of the MG dye by Fe_3O_4@SiO_2 catalyst under near neutral environment. Overall, the entire process of fenton-like degradation of MG dye by Fe_3O_4@SiO_2 catalyst can be explained by the following reaction pathways.[49,50]

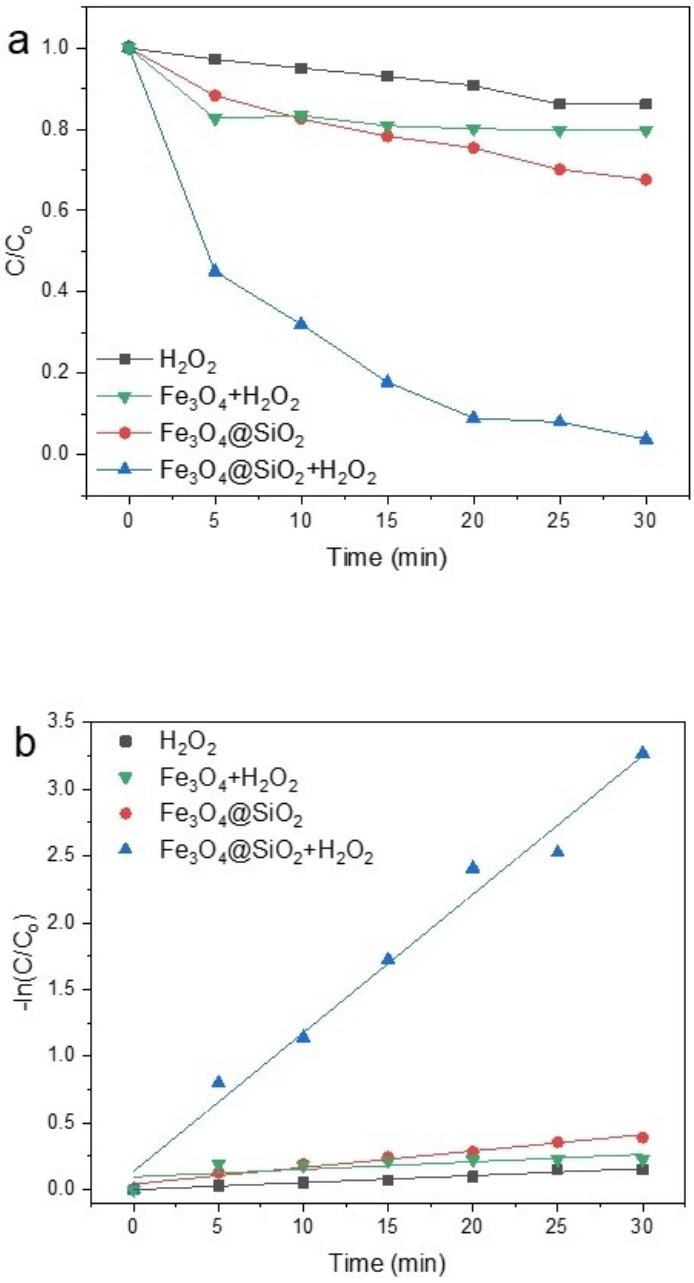

Figure 7. a) Degradation efficiencies and b) kinetics analysis of Malachite Green Dye in different systems.

1. Preconcentration of MG dye on SiO_2 shell of Fe_3O_4@SiO_2 nano-catalyst via adsorption.

$$\mathbf{MG + Fe_3O_4@SiO_2 \longrightarrow MG\text{-}Fe_3O_4@SiO_2} \quad (2)$$

2. Formation of hydroxyl and hydroperoxyl radicals by the Iron oxide cores.

$$\mathbf{Fe_3O_4 + H^+ \longrightarrow Fe^{2+}/Fe^{3+} + {\cdot}H_2O} \quad (3)$$

$$\mathbf{Fe^{2+} + H_2O_2 \longrightarrow Fe^{3+} + HO^- + {\cdot}{}^*OH} \quad (4)$$

$$\mathbf{Fe^{3+} + H_2O_2 \longrightarrow Fe^{2+} + H^+ + {\cdot}HO^*_2} \quad (5)$$

3. Degradation of MG dye via the attack of the hydroxyl radicals.

$$\mathbf{MG\text{-}Fe_3O_4@SiO_2 + {}^*OH \longrightarrow Degraded\ MG\ products} \quad (6)$$

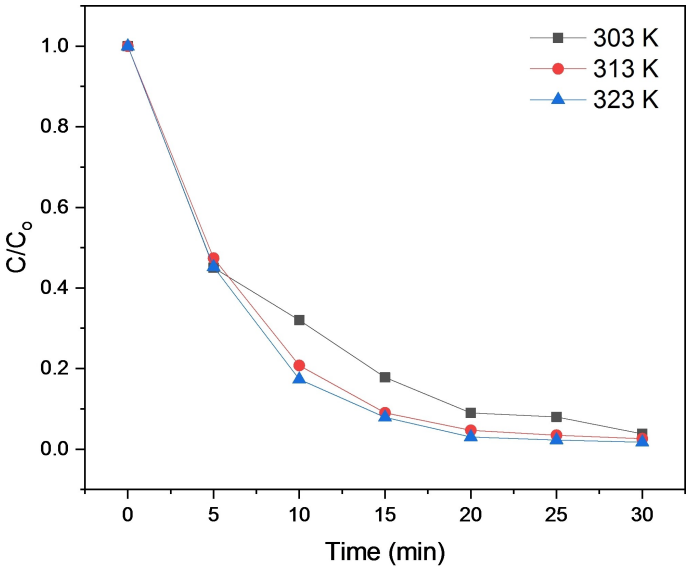

Figure 8. Effect of temperature on the Degradation efficiencies of Malachite Green Dye.

2.6. Effect of Temperature

Further studies were conducted to investigate the effect of reaction temperature on the degradation of the MG dye under optimum conditions for pH, Fe_3O_4@SiO_2 catalyst and H_2O_2 amount at three different temperatures (303 K, 313 K and 323 K). As depicted in the Figure 8, the increase in temperature resulted in a faster degradation of MG. The obtained degradation kinetics, at three temperatures are listed in Table 1. At 313 K and 323 K, around 79.24% and 82.67% of MG dye were degraded within the first 10 minutes, respectively. By 15 minutes, more than 90% of the dye was degraded at the elevated temperatures. While at reaction temperature of 303 K, only 68% of the dye were removed within the first 10 minutes and by 15 minutes it improved to 82.18%. However, at the end of the 30 minutes, only slight improvement in the degradation efficiencies are observed (96.18%, 97.76% and 98.28% at 303 K, 313 K and 323 K, respectively). The faster degradation initially observed at higher temperature are mainly caused by increase in the rate of generation of Hydroxyl radicals. Elevated temperature induces the Hydrogen peroxide to react more readily with the chelated or non-chelated Ferric/Ferrous ions originating from the Fe_3O_4 cores, thereby, increasing the rate of production of hydroxyl radicals.[8,51] Moreover, the collision between the MG dye and Hydroxyl radical also increases with increase in temperature, which in turn promotes rapid degradation.[52]

Table 1. Degradation kinetics of Malachite green dye using Fe_3O_4@SiO_2 nano-catalyst.

Temp (K)	k_1 (min^{-1})
303	0.1102
313	0.1388
323	0.1522

2.7. Recyclability

One of the key factors in the application of catalyst is it stability. A catalyst that can be reused would save money and resources. Therefore, the stability and reusability of the Fe_3O_4@SiO_2 nano-catalysts were investigated by performing cyclic experiments under optimum conditions for the pH, catalyst dosage and H_2O_2 amount at 303 K. At the end of each cycle, the catalyst was separated using a magnet and reused without further treatment and the results obtained are shown in Figure 9. The degradation efficiency showed a sudden decrease to 70% in the second cycle. Further use of the catalyst, resulted in gradual decrease in the efficiency and it was below 50% by the end of the fourth cycle. The initial drop in degradation efficiency was possibly caused by the loss of active sites as the MG dye and its intermediates occupied got attached to the surface of the Fe_3O_4@SiO_2 nano-catalysts.[53] Another possible reason for the loss of degradation efficiency is the deterioration of the core-shell structure of Fe_3O_4@SiO_2 nano-catalysts which in turn may have caused a loss in Fe_3O_4.[38] Based on the results, it can be suggested that the as prepared Fe_3O_4@SiO_2 nano-catalysts can be reused for three cycles with acceptable degradation efficiency.

2.8. Comparison

The performance of the Fe_3O_4@SiO_2 in degradation of the MG dye was compared with that of the other recently reported catalysts for MG dye degradation as shown in Table 2. Based reaction rates reported, it can be seen that the Fe_3O_4@SiO_2 nano-catalyst exhibited faster kinetics compared to the ones reported for Diatomite/Manganese Silicate and Fe_2O_3/Fe_3O_4 from tea extract.[9,42] Comparing the time required to reach the maximum removal efficiency the Fe_3O_4@SiO_2 nano-catalysts took lesser time than most of the reported catalysts reported

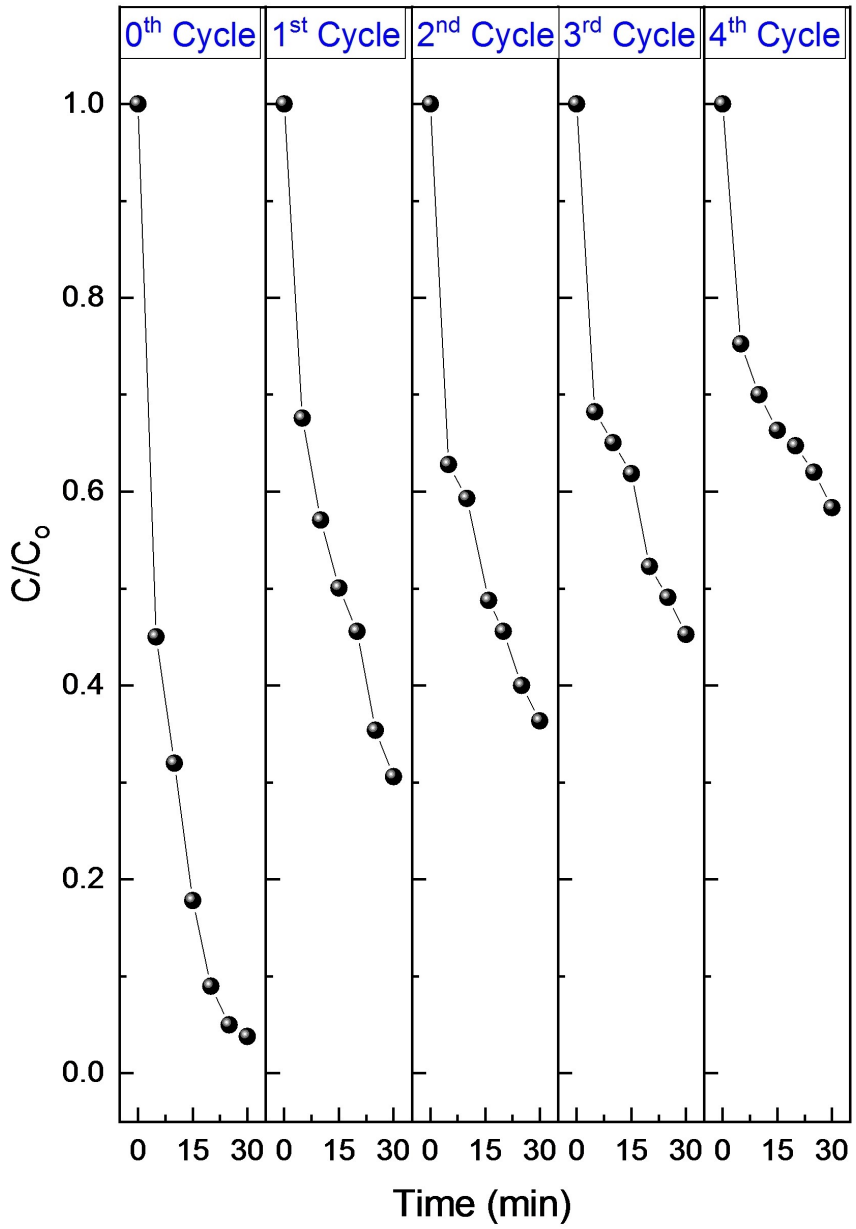

Figure 9. Recyclability performance of Fe_3O_4@SiO_2 nano-catalysts for catalytic degradation of Malachite Green dye.

Table 2. Comparison of the performance of the Fe_3O_4@SiO_2 catalyst with other recently reported catalysts for MG degradation.

Catalyst	MG conc.	pH	Dosage	Temp	H_2O_2	Time	Efficiency	k_1	Ref.
$MgFe_2O_4$	10 mg.L^{-1}	7	40 mg	303 K	0.1 mL, H_2O_2 (10%)	50 s	100%	–	[1]
Zn/HAP/$MgFe_2O_4$	10 mg.L^{-1}	3–7	40 mg	303 K	0.1 mL, H_2O_2 (10%)	2 min	100%	–	[3]
Porous Manganese Oxide Octahedral Molecular Siev (OMS-2)	5 mg.L^{-1}	–	7.5 mg	–	2.0 mL, H_2O_2 (30%)	60 min	99%	–	[54]
EDTA-Fe(iii)	10 μM	7	500 μM	293 K	20 mM	90 min	92.70%	–	[55]
Fe^{2+}	10 mg.L^{-1}	3	10 mM	313 K	25.6 mM	60 min	93.83%	–	[56]
Diatomite/Manganese Silicate	500 mg.L^{-1}	–	0.3 g/L	303 K	30 mM	70 min	93%	0.06 min^{-1}	[9]
Fe_2O_3/Fe_3O_4 from tea extract	50 mg.L^{-1}	4	0.3 g/L	308 K	7.4 mM	60 min	85%	0.0597 min^{-1}	[42]
Fe_3O_4@SiO_2	25 mg.L^{-1}	6.7	15 mg	303 K	0.05 mL, H_2O_2 (30%)	30 min	96.18%	0.1102 min^{-1}	This work

except for the ones reported for the remarkably fast $MgFe_2O_4$ and Zn/HAP/$MgFe_2O_4$.[1,3] The amount of Peroxide required to induce the fenton reactions plays a significant role in determining the cost of the degradation process. It is to be noted that the as prepared Fe_3O_4@SiO_2 nano-catalysts required 0.05 ml of H_2O_2 (30%) making it economically competitive in comparison to other catalysts.

3. Conclusions

The study showed that the potentials of Fe_3O_4@SiO_2 as a catalyst to degrade malachite green (MG) dye from aqueous solutions. The core-shell Fe_3O_4@SiO_2 nano-catalysts were successfully synthesized by a combination of Solvothermal and sol-gel technique. The as prepared nano-catalyst were then characterized using the XRD, FTIR, SEM-EDX, TEM and VSM studies to confirm the presence of all the desired elements and the core-shell morphology of the Fe_3O_4@SiO_2 nano-catalysts as well as its magnetic properties. fenton-like degradation experiments were then performed to investigate the effectiveness of the nano-catalysts in degrading of 25 mg.L^{-1} of MG dyes. The optimum conditions for the pH, catalyst dosage and H_2O_2 amount for the degradation process was determined to be 6.7, 15 mg and 50 μL, respectively. Under the optimized conditions, 96.18% of the MG dye degraded within 30 minutes of reaction time at 303 K. Owing to their magnetic properties, the as prepared nano-catalyst could be easily recovered and reused with acceptable cyclic performance. Overall, the findings of this work showed the significance of core-shell Fe_3O_4@SiO_2 nano-catalysts for its application in degradation MG dye, adding to its potential as a catalyst for environmental remediation applications.

4. Declarations

4.1. Availability of data and material

Available upon request

4.2. Code availability

NA

Supporting Information Summary

The supporting information provides the experimental details associated with the research work. It includes necessary details regarding all the required precursors as well as the steps involved for the synthesis of heterogeneous Fe_3O_4@SiO_2 nanocomposites using a combination of hydrothermal and sol-gel technique. As mentioned earlier, the prepared nanocomposites were characterized using various techniques and the details of the instruments used for each of the characterization technique are also provided. Finally, the experimental procedure followed for the catalytic degradation of the Malachite green dye using heterogeneous Fe_3O_4@SiO_2 nanocomposites as well as different equations used to calculate the removal efficiency and kinetics are described in the supporting information.

Acknowledgments

This research was made possible by an NPRP Grant#10-0127-170270 from the Qatar National Research Fund (a member of Qatar Foundation). The statements made herein are solely the responsibility of the authors. The authors would like to acknowledge the help Centre for Advanced Materials (CAM) at Qatar University and Mr. Abdullah Al Ashraf for providing XRD test data. SEM/EDX tests was accomplished in the Central Laboratories unit, Qatar University.

Conflict of Interest

The authors declare no conflict of interest.

Keywords: Dye · Fenton-degradation · Fe_3O_4@SiO_2 · Heterogeneous catalysis · Malachite green · Nanoparticles.

[1] K. C. Das, S. S. Dhar, *J. Alloys Compd.* **2020**, *828*, 154462.
[2] T. Fazal, A. Mushtaq, F. Rehman, A. U. Khan, N. Rashid, W. Farooq, M. S. U. Rehman, J. J. R. Xu, *Renewable Sustainable Energy Rev.* **2018**, *82*, 3107–3126.
[3] K. C. Das, S. S. Dhar, *J. Mater. Sci.* **2020**, *55*, 4592–4606.
[4] W. Cheng, S.-G. Wang, L. Lu, W.-X. Gong, X.-W. Liu, B.-Y. Gao, H.-Y. Zhang, *Biochem. Eng. J.* **2008**, *39*, 538–546.
[5] S. Meena, D. Vaya, B. K. Das, *Bull. Mater. Sci.* **2016**, *39*, 1735–1743.
[6] B. R. Vergis, R. Hari Krishna, N. Kottam, B. M. Nagabhushana, R. Sharath, B. Darukaprasad, *J. Nanostruct. Chem.* **2018**, *8*, 1–12.
[7] K. V. K. Rao, *Toxicol. Lett.* **1995**, *81*, 107–113.
[8] B. H. Hameed, T. W. Lee, *J. Hazard. Mater.* **2009**, *164*, 468–472.
[9] D. B. Jiang, Y. Yuan, D. Zhao, K. Tao, X. Xu, Y. X. Zhang, *J. Nanopart. Res.* **2018**, *20*, 123.
[10] G. Subramanian, G. Madras, *Water Res.* **2016**, *104*, 168–177.
[11] P. P. Marcinowski, J. P. Bogacki, J. H. Naumczyk, *J. Environ. Sci. Health Part A* **2014**, *49*, 1531–1541.
[12] S.-T. Yang, W. Zhang, J. Xie, R. Liao, X. Zhang, B. Yu, R. Wu, X. Liu, H. Li, Z. Guo, *RSC Adv.* **2015**, *5*, 5458–5463.
[13] S. Caudo, G. Centi, C. Genovese, S. Perathoner, *Top. Catal.* **2006**, *40*, 207–219.
[14] N. N. Tušar, D. Maučec, M. Rangus, I. Arčon, M. Mazaj, M. Cotman, A. Pintar, V. Kaučič, *Adv. Funct. Mater.* **2012**, *22*, 820–826.
[15] J. L. Wang, L. J. Xu, *Crit. Rev. Environ. Sci. Technol.* **2012**, *42*, 251–325.
[16] P. V. Nidheesh, *RSC Adv.* **2015**, *5*, 40552–40577.
[17] S. Rahim Pouran, A. A. Abdul Raman, W. M. A. Wan Daud, *J. Cleaner Prod.* **2014**, *64*, 24–35.
[18] J. He, X. Yang, B. Men, D. J. J. o. e. s. Wang, *J. Environ. Sci.* **2016**, *39*, 97–109.
[19] R. Huang, Z. Fang, X. Yan, W. Cheng, *Chem. Eng. J.* **2012**, *197*, 242–249.
[20] J. Liu, J. Zhou, Z. Ding, Z. Zhao, X. Xu, Z. Fang, *Ultrason. Sonochem.* **2017**, *34*, 953–959.
[21] B. da Costa Carvalho, F. C. Andrade Corbi, F. A. Sigoli, I. O. Mazali, *RSC Adv.* **2016**, *6*, 38617–38623.
[22] X. Zhang, M. He, J.-H. Liu, R. Liao, L. Zhao, J. Xie, R. Wang, S.-T. Yang, H. Wang, Y. Liu, *Chin. Sci. Bull.* **2014**, *59*, 3406–3412.
[23] R. Wang, X. Liu, R. Wu, B. Yu, H. Li, X. Zhang, J. Xie, S.-T. Yang, *RSC Adv.* **2016**, *6*, 8594–8600.
[24] X. Liu, Q. Zhang, B. Yu, R. Wu, J. Mai, R. Wang, L. Chen, S.-T. Yang, *Catalysts* **2016**, *6*, 146.
[25] L. Wang, Y. Shi, H. Zhang, X. Bai, Y. Wang, T. J. J. o. M. C. A. Ma, *J. Mater. Chem. A* **2014**, *2*, 15279–15283.
[26] P. J. N. G. W. G. Scherrer, *Nachr. Ges. Wiss* **1918**, *2*, 96–100.

[27] J. Arenas-Alatorre, S. C. Tehuacanero, O. Lukas, A. Rodríguez-Gómez, R. Hernández Reyes, C. Tapia-del León, J. V. Lara, *Mater. Lett.* **2019**, *242*, 13–16.
[28] M. Abbas, S. RamuluTorati, S. A. Iqbal, C. Kim, *New J. Chem.* **2017**, *41*, 2724–2734.
[29] Y. Xu, Y. Zhou, W. Ma, S. Wang, *J. Nanomater.* **2013**, *2013*, 178138.
[30] X. Du, J. He, J. Zhu, L. Sun, S. An, *Appl. Surf. Sci.* **2012**, *258*, 2717–2723.
[31] J. Zhang, M. Liu, Z. Liu, T. Yang, Q. He, K. Yang, H. Wang, *J. Sol-Gel Sci. Technol.* **2017**, *82*, 424–431.
[32] S. Rostamnia, B. Gholipour, X. Liu, Y. Wang, H. Arandiyan, *J. Colloid Interface Sci.* **2018**, *511*, 447–455.
[33] M. Ergüt, D. Uzunoğlu, A. Özer, *Part A: Environ. Sci. Eng.* **2019**, *54*, 786–800.
[34] H. Zheng, H. Zhang, X. Sun, P. Zhang, T. Tshukudu, G. Zhu, *Water Sci. Technol.* **2010**, *62*, 1304–1311.
[35] D. Ghime, P. Goru, S. Ojha, P. Ghosh, *Global NEST J.* **2019**, *21*, 195–203.
[36] X. Liu, C. Sun, L. Chen, H. Yang, Z. Ming, Y. Bai, S. Feng, S.-T. Yang, *Mater. Chem. Phys.* **2018**, *213*, 231–238.
[37] X. Xue, K. Hanna, C. Despas, F. Wu, N. J. J. o. M. C. A. C. Deng, *J. Mol. Catal. A* **2009**, *311*, 29–35.
[38] D. B. Jiang, X. Liu, X. Xu, Y. X. Zhang, *J. Phys. Chem. Solids* **2018**, *112*, 209–215.
[39] M. S. Lucas, J. A. Peres, *Dyes Pigm.* **2006**, *71*, 236–244.
[40] S. Thakur, M. J. I. R. J. E. T. Chauhan, *Int. Res. J. Eng. Technol.* **2016**, *3*, 254–259.
[41] Z. Wang, H. Yu, Y. Xiao, L. Zhang, L. Guo, L. Zhang, X. J. C. E. J. Dong, *Chem. Eng. J.* **2020**, *394*, 125014.
[42] Y. Wu, S. Zeng, F. Wang, M. Megharaj, R. Naidu, Z. Chen, *Sep. Purif. Technol.* **2015**, *154*, 161–167.
[43] X. Wu, Z. Nan, *Mater. Chem. Phys.* **2019**, *227*, 302–312.
[44] S. S. F. Carvalho, N. M. F. Carvalho, *J. Environ. Manage.* **2017**, *187*, 82–88.
[45] Y. Xu, Y. Zhou, W. Ma, S. Wang, S. Li, *J. Nanopart. Res.* **2013**, *15*, 1716.
[46] N. Bayal, P. Jeevanandam, *J. Nanopart. Res.* **2013**, *15*, 2066.
[47] D. Colón, E. J. Weber, J. L. Anderson, *Environ. Sci. Technol.* **2008**, *42*, 6538–6543.
[48] S.-H. Kang, W. Choi, *Environ. Sci. Technol.* **2009**, *43*, 878–883.
[49] Z. Diao, M. Li, F. Zeng, L. Song, R. Qiu, *J. Hazard. Mater.* **2013**, *260*, 585–592.
[50] E. Kusvuran, O. Gulnaz, A. Samil, Ö. J. J. o. h. m. Yildirim, *J. Hazard. Mater.* **2011**, *186*, 133–143.
[51] J.-H. Sun, S.-P. Sun, G.-L. Wang, L.-P. Qiao, *Dyes Pigm.* **2007**, *74*, 647–652.
[52] P. Guo, L. Cui, Y. Wang, M. Lv, B. Wang, X. S. Zhao, *Langmuir* **2013**, *29*, 8997–9003.
[53] A. A. Babaei, A. Azari, R. R. Kalantary, B. Kakavandi, *Water Sci. Technol.* **2015**, *72*, 1988–1999.
[54] M. Hajnajafi, A. Khorshidi, A. G. Gilani, B. Heidari, *Res. Chem. Intermed.* **2018**, *44*, 3313–3323.
[55] Y. Hu, Y. Li, J. He, T. Liu, K. Zhang, X. Huang, L. Kong, J. Liu, *J. Environ. Manage.* **2018**, *226*, 256–263.
[56] A. Elhalil, H. Tounsadi, R. Elmoubarki, F. Z. Mahjoubi, M. Farnane, M. Sadiq, M. Abdennouri, S. Qourzal, N. Barka, *Water Resour. Ind.* **2016**, *15*, 41–48.

Submitted: October 13, 2020
Accepted: January 3, 2021